Clim. Past Discuss., 10, 4385–4424, 2014
www.clim-past-discuss.net/10/4385/2014/
doi:10.5194/cpd-10-4385-2014

Climate of the Past
Discussions
Open Access

High resolution leaf wax carbon and hydrogen isotopic record of late Holocene paleoclimate in arid Central Asia

B. Aichner[1,2], S. J. Feakins[1], J. E. Lee[3], U. Herzschuh[2,4], and X. Liu[5]

[1]University of Southern California, Los Angeles, USA
[2]University of Potsdam, Potsdam, Germany
[3]Brown University, Providence, USA
[4]Alfred-Wegener-Institute, Potsdam, Germany
[5]Capital Normal University, Beijing, China

Received: 2 October 2014 – Accepted: 24 October 2014 – Published: 21 November 2014

Correspondence to: B. Aichner (bernhard.aichner@gmx.de)

Published by Copernicus Publications on behalf of the European Geosciences Union.

Abstract

Central Asia is located at the intersection of large scale atmospheric circulation systems. It is thus likely to be highly susceptible to changes in the dynamics of those systems, however little is still known about the regions paleoclimate history. Here we present carbon and hydrogen isotopic compositions of *n*-alkanoic acids from a late Holocene sediment core from Lake Karakuli (eastern Pamir, Xinjiang Province, China). Instrumental evidence and isotope-enabled climate model experiments with the Laboratoire de Météorologie Dynamique Zoom model version 4 (LMDZ4) demonstrate that δD values of precipitation in the region are influenced by both temperature and precipitation amount. We find that those parameters are inversely correlated on an annual scale; i.e. climate varies between cool/wet and dry/warm over the last 50 years. Since the isotopic signals of these changes are in the same direction and therefore additive, isotopes in precipitation are sensitive recorders of climatic changes in the region. Additionally, we infer that plants are using year round precipitation (including snow-melt) and thus leaf wax δD values must also respond to shifts in the proportion of moisture derived from westerly storms during late winter/early spring. Downcore results give evidence for a gradual shift to cooler and wetter climates between 3.5 and 2.5 cal kyr BP, interrupted by a warm/dry episode between 3.0–2.7 kyr BP. Further cool and wet episodes occur between 1.9–1.5 kyr BP and between 0.6–0.1 kyr BP, the latter coeval with the Little Ice Age. Warm and dry episodes between 2.5–1.9 kyr BP and 1.5–0.6 kyr BP coincide with the Roman Warm Period and Medieval Climate Anomaly, respectively. Finally, we find a drying tend in recent decades. Regional comparisons lead us to infer that the strength and position of the Westerlies, and wider Northern Hemispheric climate dynamics control climatic shifts in arid Central Asia.

CPD
10, 4385–4424, 2014

1 Introduction

Future climate change associated with anthropogenic disturbance of the Earth system is expected to go in hand with changes in atmospheric circulation dynamics (Seth et al., 2011). In this scenario, certain regions of the Earth are thought to be susceptible to severe and likely abrupt changes in moisture delivery and temperature. One such region is Central Asia, located at the intersection of influences from the mid-latitude Westerlies, the Siberian High, and the limits of the Indian Monsoon (Aizen et al., 2001; Chen et al., 2008). However, the nature and magnitude of the changes, as well as their regional effects are still poorly known. Detailed knowledge about past naturally-driven climate variability in this region can contribute to a better understanding of the complex atmospheric circulation system, which can in turn help to better predict possible impacts of future anthropogenically-driven climate changes.

While a large number of studies have analysed climate dynamics in monsoonal eastern Asia and the north- and southeastern Tibetan Plateau (e.g. reviewed in Morill et al., 2003; An et al., 2006; Herzschuh, 2006), the density of paleoclimatic records in continental Central Asia remains comparably low. Central Asian records include studies of glacial extent in the Pamir (e.g. Narama, 2002a, b) and tree-ring width reconstructions (e.g. Esper et al., 2002; Treydte et al., 2006). Lacustrine sedimentary archives exist from Kyrgyzstan (Ricketts et al., 2001; Lauterbach et al., 2014; Mathis et al., 2014), the Aral Sea (Sorrell et al., 2007a, b; Boomer et al., 2009; Huang et al., 2011), the Western and Southern Tarim Basin (Zhao et al., 2012; Zhong et al., 2007), and the Pamirs/Tajikistan (Mischke et al., 2010c; Lei et al., 2014) (Fig. 1b). Only one of those studies has included compound specific hydrogen isotopic analyses (Lauterbach et al., 2014), which have elsewhere in Asia shown its potential to provide information about moisture sources, precipitation amount and temperature (Mügler et al., 2010; Aichner et al., 2010c; Liu et al., 2008).

Climatic patterns in Central Asia are complex due to the boundary location between various large-scale atmospheric circulation systems as well as the topography of the

CPD
10, 4385–4424, 2014

area (Fig. 1). While the easternmost parts are generally arid and receive most of their precipitation during the summer, western regions receive higher proportional input from Westerly-derived winter precipitation (Miehe et al., 2001; Machalett et al., 2008; Lauterbach et al., 2014). Thus a dense network of paleoclimatic records is required to fully understand spatial patterns of climate dynamics over time.

To further decipher past climatic processes in our study we generated a high-resolution, mid to late Holocene paleoclimatic record from Lake Karakuli (western China), located in the eastern Pamir mountain range, at the very westernmost edge of the Tibetan Plateau. Building upon the work of Liu et al. (2014) who inferred glacial fluctuations from grain-size parameters and elemental composition at the same lake, we use compound-specific carbon ($\delta^{13}C$) and hydrogen (δD) isotopic compositions of long-chain ($> C_{24}$) *n*-alkanoic acids originating from plant leaf waxes to deduce past climatic changes in our study area. To evaluate the hydrogen isotopic data it is essential to understand what drives the variability of the isotopic signal which is recorded by the biomarker in a specific study area. Therefore we draw comparisons to isotope-enabled model experiments using the Laboratoire de Météorologie Dynamique Zoom model version 4 (LMDZ4) simulations (Hourdin et al., 2006; Risi et al., 2010, 2012a, b; Lee et al., 2012). On basis of this data we characterize the processes controlling isotopic composition of precipitation over Central Asia and discuss the implications for the interpretation of the biomarker isotopic evidence.

2 Study site

Lake Karakuli (also: Lake Kala Kule) is a small lake (ca. 1 km × 1.5 km) located at the westernmost edge of Xinjiang Province (PR China) at an altitude of 3650 m, between the massifs of Kongur Shan and Muztagh Ata, both exceeding 7500 m (Fig. 1a). Those mountains which form the eastern edge of the Pamir plateau and the very westernmost edge of the Tibetan Plateau are directly adjacent to the mountain ranges of Karakorum and Tien Shan. The climate in this high altitude region is cold and dry. At Taxkorgan

CPD
10, 4385–4424, 2014

climate station, 80 km south of Lake Karakuli (3090 m), average annual temperatures and precipitation amounts are 3.2 °C and 69 mm, respectively (1957–1990; Miehe et al., 2001) with June and July being the wettest months. Climatic data from Bulon Kol (3310 m), 30 km north of our study area, are in a similar range (0.6 °C and 127 mm) with a precipitation maximum during spring and summer (1956–1986; Miehe et al., 2001). At higher altitudes, precipitation amounts increase by orographic forcing. At the Muztagh Ata, annual rain- and snowfall was estimated to account for about 300 mm at the glacier accumulation zone (at 5919 m; Seong et al., 2009a) while other studies estimated a water equivalent depth of 605 mm for snow accumulation at 7010 m (Wu et al., 2008).

Lake Karakuli is an open freshwater lake with a maximum depth of 20 m. The relatively small catchment comprises meltwater mainly derived from glaciers on the western flank of Mt. Muztagh Ata. Those form an alluvial fan with several creeks which discharge into the lake from the south while the single outflow drains towards the north (see Figs. 1 and S1 in the Supplement). Most of the glacial runoff derived from the surrounding massifs incl. the main glacier of Muztagh Ata and Mt Kongur Shan does currently not discharge into the lake.

The sparse vegetation consists of alpine grasslands, partly used for pasture (see Fig. S1), with alpine desert at higher altitudes. Above 5500 m the landscape is fully glaciated (with valley glaciers descending to 4300 m; Tian et al., 2006). Compared to other shallow lakes on the Tibetan Plateau where macrophytes are numerous (Aichner et al., 2010b), there are only a few emergent and submerged macrophytes on or close to the shores, and few indications for submerged plants in the deeper parts of the lake.

CPD
10, 4385–4424, 2014

3 Material and methods

3.1 Coring and chronology

A sediment core with a composite length of ca. 820 cm was taken in September 2008 at 38.43968° N and 75.05725° E from a water depth of 16 m, using an UWITEC coring system and a floating platform. The chronology was based-on seventeen radiocarbon ages derived from ^{14}C AMS dating conducted on total organic carbon (TOC) (Liu et al., 2014). The 0 cal yr BP (1950 AD) was derived from $^{210}PB/^{137}Cs$ dating and appeared at ca. 10.5 cm depth. A reservoir-effect of 1880 years was extrapolated from dating of core-top samples and assumed to be constant throughout the core. The ^{14}C-ages indicate a nearly constant sedimentation rate across 4.3 kyr. For calibration of the ages and construction of the age-depth model the IntCal09 dataset was used (Reimer et al., 2009) applying a Bayesian method (Blaauw and Christen, 2011); for details see Liu et al. (2014).

3.2 Lab chemistry

Sediments were extracted with Accelerated Solvent Extraction system (ASE 350; Dionex), under high pressure (1500 psi) and temperature (100 °C) and using DCM/MeOH (9 : 1) as solvent. Alkanoic acids were separated from the total lipid extract using column chromatography (5 cm × 40 mm Pasteur pipette, NH_2 sepra bulk packing, 60 Å), eluting with 2 : 1 DCM/isopropanol, followed by 4 % formic acid in diethylether, yielding neutral and acid fractions respectively. The acid fraction was esterified with 5 % HCl and 95 % methanol (of known isotopic composition) at 70 °C for 12 h to yield corresponding fatty acid methyl esters (FAMEs). Lipids were obtained by liquid–liquid extraction using hexane as the non-polar solvent, and dried by passing through a column of anhydrous Na_2SO_4. They were further purified using column chromatography (5 cm × 40 mm Pasteur pipette, 5 % water-deactivated silica gel, 100–200 mesh), eluting with hexane, followed by FAMEs eluted with DCM.

CPD
10, 4385–4424, 2014

3.3 Biomarker isotopic analysis

Compound specific isotopic values were obtained using gas chromatography isotope ratio mass spectrometry (GC-IRMS). We used a Thermo Scientific® Trace gas chromatograph equipped with a Rxi-5 ms column (30 m × 0.25 mm, film thickness 1 µm) and a programmable temperature vaporizing (PTV) injector operated in solvent split mode with an evaporation temperature of 60 °C. The GC was connected via a GC Isolink with pyrolysis/combustion furnace (at 1400/1000 °C) and a Conflo IV interface to a DeltaV$_{Plus}$ isotope ratio mass spectrometer. The H_3^+-factor (Sessions et al., 2001) was determined daily to test measurement-linearity of the system and accounted for 5.8 ppm mv^{-1} on average. Reference peaks of H_2/CO_2 bracket *n*-alkanoic acid peaks during the course of a GC-IRMS run; two of these peaks were used for standardization of the isotopic analysis, while the remainders were treated as unknowns to assess precision. Except for the case of co-elution, precision of these replicates was better than 0.6 ‰.

Data were normalized to the Vienna Standard Mean Ocean Water (VSMOW)-Standard Light Antarctic Precipitation (SLAP) hydrogen isotopic scale and to Vienna Pee Dee Belemnite (VPBD) carbon isotopic scale by comparing with an external standard containing 15 *n*-alkane compounds (C_{16} to C_{30}) of known isotopic composition (obtained from A. Schimmelmann, Indiana University, Bloomington). The RMS error of replicate measurements of the standard across the course of analyses was below 5 ‰ (hydrogen) and 0.7 % (carbon) For hydrogen isotopes we further monitored for instrument drift by measuring the δD values of a C_{34} *n*-alkane internal standard co-injected with the sample (−240.6 ± 3.0 ‰; $n = 105$). The isotopic composition of H and C added during methylation of alkanoic acids was estimated by methylating and analyzing phthalic acid as a dimethyl ester (isotopic standard from A. Schimmelmann, University of Indiana) yielding $\delta D_{methanol} = -198.3 \pm 3.9$ ‰, $\delta^{13}C_{methanol} = -25.45 \pm 0.42$ ‰ ($n = 7$). Correction for H and C added by methylation was then made by way of mass balance.

CPD
10, 4385–4424, 2014

3.4 LMDZ4 simulations

To understand the control of spatial and seasonal isotopic variations, we use the climate model LMDZ4 (Hourdin et al., 2006) to characterize the processes controlling isotopes of precipitation over our study area. Details about the model and methodology are described in Risi et al. (2010, 2012a, b) and Lee et al. (2012). Briefly, the applied model version incorporates the entire cycle of stable water isotopes and includes fractionation when phase changes occur. The resolution of the model is $2.5^\circ \times 3.75^\circ$ with 19 vertical levels in the atmosphere. To obtain more realistic simulations of the hydrology and isotope values compared with free-running simulations and to better reproduce the observed circulation pattern, simulated winds from LMDZ4 are relaxed toward the pseudo-observed horizontal wind field from the ERA-40 reanalysis results (Uppala et al., 2005) with a time constant of 1 h. Boundary conditions used observed sea surface temperatures and sea ice fractions from the HadISST data set (Rayner et al., 2003) from 1958 to 2009.

4 Results

4.1 Lipid concentrations

Due to the sparse vegetation in and around the lake, concentrations of leaf wax biomarkers in the sediments were relatively low. For compound -specific isotopic analysis we chose fatty acids (FAs) which showed higher concentrations than alkanes in a set of test samples. Here, C_{24}, C_{26} and C_{28} *n*-alkanoic acids were the most abundant compounds, which average concentrations of ca. 1050, 1000 and 750 $ng\,g^{-1}$ dw (nanograms per grams dry weight; Fig. S2). We found fatty acid concentrations were relatively constant with depth, suggesting no major change in productivity, dilution or preservation during the late Holocene.

4.2 δD and $\delta^{13}C$ values of leaf wax lipids and water samples

In total, we measured 125 core samples for hydrogen isotopic composition and 66 samples for carbon isotopic composition (Table S6). Samples contained C_{16}-C_{28} *n*-alkanoic acids with an even:odd chain length preference. We report isotopic results for the C_{24}, C_{26} and C_{28} *n*-alkanoic acids as these are target long chain compounds within the dynamic range of isotopic measurement capabilities (Table S6, Fig. S3).

$\delta^{13}C$ values are generally more depleted with increasing chain-length, with C_{24} averaging to -27.9 ± 1.4 ‰ and C_{26} to -29.3 ± 1.0 ‰; and C_{28} *n*-alkanoic acids to -31.0 ± 0.9 ‰ (Figs. 2 and S3). For the C_{28} we find no significant downcore trend. C_{24} shows the largest variations in $\delta^{13}C$ values with generally more ^{13}C-depleted values in the middle of the core (min: -30.7 ‰) compared to the core-base and core-top (max: -24.3 ‰) (Fig. S3). For hydrogen isotopes, compounds are also more *D*-depleted with increasing chain-length (C_{24}: -173 ± 6 ‰; C_{26}: -182 ± 7 ‰; C_{28}: -185 ± 6 ‰; Fig. 2). We observe downcore variations in δD values for C_{26} and C_{28} ranging from -196 to -167 ‰.

Six water samples (two from inflows, two from Lake Karakuli and two from ponds nearby) have been analysed for isotopic composition (Table 1). Both inflows show similar isotopic signatures (ca. -83 ‰). The lake water averages $+3.5$ ‰ ($\delta^{18}O$) and $+15$ ‰ (δD) enriched relative to the inflow due to evaporation. Closed ponds nearby are also evaporatively enriched relative to inflow.

CPD
10, 4385–4424, 2014

5 Discussion

5.1 Origin of organic compounds and implications for source water

5.1.1 Molecular abundance distribution

Organic compounds in lake sediments originate from a mixture of terrestrial and aquatic organisms, with molecular abundance distributions and isotopic compositions that may be diagnostic of source. Most plants contain a broad of range of biomarkers (e.g. *n*-alkanes or fatty acids) but the fingerprints of the different compound classes are mainly dominated by compounds of a specific chain-length. Terrestrial and emergent aquatic plants for instance produce higher proportional abundances of long-chain *n*-alkanes (e.g. C_{29} and C_{31}) while submerged macrophytes contain higher amounts of mid-chain *n*-alkanes (e.g. C_{23} and C_{25}) (Ficken et al., 2000; Aichner et al., 2010b). *n*-Alkanoic acids show a less distinct pattern (Ficken et al., 2000), but also here long-chain compounds (e.g. C_{28}-FAs) are mostly interpreted to be originated from terrestrial sources (e.g. Kusch et al., 2010; Feakins et al., 2014).

In the sediments of Lake Karakuli the contribution of aquatic plants to the lipid pool is considered to be relatively low compared to other Tibetan high altitude lakes. A plant sample collected close to the shore-line (ca. 20 cm water depth) shows a strong dominance of C_{16} and C_{18}-FAs and minor relative amounts of C_{20} to C_{30} even-chain FAs (see Fig. S4). This fatty acid-pattern is in agreement with published fingerprints of other aquatic plants collected on the Tibetan Plateau (Wang and Liu, 2012). Hence, the low relative abundance of C_{16} and C_{18}-FAs in our sediment samples suggests a relatively low contribution of plant material derived from aquatic macrophytes to the organic matter in Lake Karakuli, at least at the position where the sediment core was taken.

CPD
10, 4385–4424, 2014

Late Holocene paleoclimate in arid Central Asia

B. Aichner et al.

Title Page
Abstract Introduction
Conclusions References
Tables Figures
◂◂ ▸▸
◂ ▸
Back Close
Full Screen / Esc
Printer-friendly Version
Interactive Discussion

5.1.2 Carbon isotopic signal

Additional indication for the source of compounds comes from their carbon isotopic signature. Lipids of terrestrial C_3-plants usually show values around −30 to −35 ‰, while compounds derived from terrestrial C_4-plants and from submerged aquatic macrophytes can reach significantly more enriched values in the range −15 to −20 ‰ (Chikaraishi and Naraoka, 2005; Aichner et al., 2010). The difference between C_3 and C_4-plants can be explained by different isotopic fractionation in carbon assimilation of those two plant types, while the enriched values of submerged aquatic plants are due to the uptake of different carbon sources i.e. isotopically enriched bicarbonate instead of dissolved CO_2 (Allen and Spence, 1981; Prins and Elzenga, 1989).

As a consequence, in regions where C_4-vegetation is widely absent, as in high-altitude regions of the Tibetan Plateau and bordering mountains, the carbon isotopic signature of biomarkers can be applied to distinguish between aquatic and terrestrial sources (Aichner et al., 2010a, b). In our sediment core from Lake Karakuli $\delta^{13}C$ values of the C_{28}-FA are similar to that of terrestrial C_3-plants without a clear trend (Figs. 2 and S3). Thus, we conclude that this compound is predominantly derived from terrestrial C_3 grasses in the lake catchment. $\delta^{13}C$ values of C_{24} and C_{26}-*n*-alkanoic acids are slightly higher than for C_{28}, indicating an increasing contribution of submerged aquatic plant material with decreasing chain lengths.

$\delta^{13}C$ values of C_{24} *n*-alkanoic acids are controlled by relative contributions of aquatic macrophytes and/or macrophyte productivity, with higher productivity leading to higher $\delta^{13}C$ values (Aichner et al., 2010b). We hypothesize that higher proportional input of aquatic material to the sedimentary organic matter is indicative of warmer and possibly also drier conditions. Longer ice-free periods and a lower lake level could be the driving factors behind enhanced macrophyte growth during warmer years. We estimate the macrophyte contribution to the lipid pool on basis of a simple binary isotopic model with −19 ‰ as average end-member value for aquatic lipids (Aichner et al., 2010a) and −33 ‰ for terrestrial lipids (Ficken et al., 2000) (Fig. 7).

CPD
10, 4385–4424, 2014

5.1.3 Hydrogen isotopic signal

Hydrogen isotopes provide further evidence for the origins of C_{24} and C_{26} or C_{28} *n*-alkanoic acids. The average δD values of C_{24} are ca. 9–12 ‰ higher than that of C_{26} and C_{28} (Fig. 2). A different water source i.e. isotopically enriched lake water (see Table 1) instead of water derived from precipitation or snow-melt could explain this. We assume that C_{24} is derived from a mixed source which could be both aquatic and terrestrial, while C_{28} and also C_{26} can be considered as of mainly terrestrial origin.

The δD values of these terrestrial biomarkers is representative of the hydrogen isotopic composition of the source water which – for terrestrial plants – could be expected to be spring and summer precipitation during the growing season (Sachse et al., 2012), although a contribution of *D*-depleted melt-water from snow in the early spring growth period is highly likely (Fan et al., 2013). The fractionation between source water (i.e. leaf water) and lipids are variable but previous studies found that for terrestrial C_3-grasses they average to -149 ± 28 ‰ ($n = 47$) for the C_{29} *n*-alkane (Sachse et al., 2012). In arid ecosystems, soil-water evaporation (for grasses; Smith and Freeman, 2006) and transpiration from the leaf, lead to isotopic enrichment of leaf water above the meteoric water (Feakins and Sessions, 2010; Kahmen et al., 2013a and b). Recent results from the Central Tibetan Plateau, which is a similar environmental setting to our study, quantified the apparent isotopic fraction between meteoric water and *n*-alkanes to be ca. −95 ‰ due to ca. +70 ‰ evapotranspirational isotopic enrichment of the meteoric water (Günther et al., 2013). This is in agreement with the average fractionation from Feakins and Sessions (2010) who suggested ca. −95 ‰ as net fractionation factor between meteoric water and leaf wax *n*-alkanes in an arid ecosystem (southern California), and found similar values for *n*-alkanoic acids in a later study from that region (Feakins et al., 2014).

While the fractionation was not directly determined on modern plant *n*-alkanoic acids in this catchment, based on core-top δD_{lipid} values of ca. −190 ‰ and knowledge of hydrogen isotope values of modern precipitation and waters in the catchment we can infer a reasonable catchment average apparent fractionation (Fig. 3). Summer precipitation in the catchment averages ca. −45 ‰ at Lake Karakuli, compared to mean annual precipitation average of ca. −90 ‰ (derived from the Online Isotopes in Precipitation Calculator; Bowen and Revenaugh, 2013; Fig. 4b). Assuming the summer precipitation is indicative of source water, and then given the OIPC summer precipitation δD value of −45 ‰ and the measured sedimentary value of C_{28} *n*-alkanoic acids (−190 ‰) we would compute an apparent fractionation of ca. −150 ‰ (see Fig. S5 for formula to calculate isotopic fractionation factors). Whereas if we use mean annual precipitation (ca. −90 ‰; OIPC) then the calculated apparent fractionation would be ca. −110 ‰ which is closer to the reported fractionation factors for arid ecosystems (Feakins and Sessions, 2010; Günther et al., 2013).

The δD values of the two lake inflows sampled in September 2008 (average −83 ‰; Table 1) provide a reasonable constraint on catchment average water isotopic composition in September, presumably including a mix of contributions from precipitation runoff, groundwater, and snow melt from winter precipitation and higher elevations. A calculated source water δD value based on published fractionation factors mentioned above (ca. −95 ‰) would be −110 ‰ (Fig. 3) which is in range of late-winter/early spring precipitation in the study area according to OIPC-data (Fig. 4b). These are helpful constraints on the proxy, however, regardless of knowing the exact season of source water and the appropriate fractionation which are needed for absolute isotopic conversions, we can infer relative variations in δD values of the C_{28} *n*-alkanoic acid down core in terms of variations in the δD of precipitation. We therefore use the δD values of the C_{28} and C_{26} *n*-alkanoic acids to reconstruct past variations in the isotopic composition of precipitation.

CPD
10, 4385–4424, 2014

5.2 Controls on the isotopic signature of precipitation in the eastern Pamir

5.2.1 Monthly signal

The isotopic composition of precipitation is influenced by multiple isotope effects including those associated with precipitation amount, condensation temperature, or vapour source (Gat, 1996). Beside the moisture source, in subtropical and tropical latitudes, the amount effect has usually been identified as most relevant controlling factor with lower δD values reflecting more humid episodes in sedimentary records (Schefuss et al., 2005; Tierney et al., 2008; Lee et al., 2008). At mid- and high latitudes temperature and vapour source mostly have interpreted to be the dominant factors (Dansgaard, 1964; Thompson, 2000; Rach et al., 2014).

Evaluating isotopes of precipitation in context with climatic parameters in Asia, Araguas-Araguas et al. (1998) and Yao et al. (2013) came to the conclusion that the amount effect is the dominant factor in monsoonal East Asia while in arid Central Asia temperature mainly controls δD and $\delta^{18}O$ values of precipitation. The closest meteorological stations to Lake Karakuli are the station at Bulun Kol (ca. 30 km northeast) and Taxkorgan (ca. 80 km south). Both stations record low winter precipitation and slightly enhanced amounts during the summer (Fig. 4a and b). Higher isotopic values in the summer compared to the winter (Yao et al., 2013; Bowen, 2014) suggest that monthly values are indeed driven by temperature. However, there are also small amount effect observable e.g. in June 2004 and more pronounced in June 2005 (Fig. 4a) which lowers $\delta^{18}O$ values. This gives evidence that in an integrated and weighted long-term signal the amount effect may lower the summer precipitation isotopic enrichment and dampen the seasonality of mean precipitation of isotopic values. We infer that both temperature and precipitation amount influence the mean isotopic composition of precipitation. Hence in drier years average δD values will be D-enriched relative to wetter years; and likewise warmer years will be D-enriched relative to colder years (Fig. 4b).

CPD
10, 4385–4424, 2014

5.2.2 Annual/seasonal signal

To further establish the connections between climate anomalies and isotopic signatures of precipitation in Central Asia, we compare instrumental data and climate model simulations. At Taxkorgan meteorological station we find a negative correlation between annual temperature and precipitation amount over a period of 43 yr (1957–2000; Fig. 5; data provided from Tian at al., 2006). Similar trends can be observed when comparing simulated data over a period of 50 yr (1958–2009; Fig. 5). We use the LMDZ4 climate model (Hourdin et al., 2006) to characterize the climatic processes in our study area (as described in Lee et al., 2012). We find higher annual precipitation amounts in the LMDZ4 model simulations compared to instrumental observations at Taxkorgan meteorological stations. This is related to the scale of the model resolution of $3.75^{\circ} \times 2.5^{\circ}$ (Lee et al., 2012) which includes the relatively high precipitation amounts in higher altitudes during winter (Seong et al., 2009a, b; Wu et al., 2008) within the grid box. Significant negative correlations ($r = 0.58$; $p < 0.0001$) between temperature and precipitation amount can be inferred for the summer months (April–September), while comparisons over the winter or whole year deliver non-significant correlations ($p > 0.01$; Fig. 5).

As a consequence of the negative correlation between temperature and precipitation amount we observe positive/negative correlations between precipitation isotopes and those climatic parameters for our larger study area (Fig. 6). Considering temperature, we found a positive correlation ($0.4 < r < 0.6$) for both winter and summer over large parts of Central Asia indicating the broad regional significance of our record. For the summer, no correlations are seen in India and SE Asia, where distinct monsoonal circulation and precipitation patterns exert independent controls on the isotopic values of precipitation (Morill et al., 2003; Yao et al., 2013). Considering precipitation amount, negative correlations ($-0.6 < r < -0.2$) can be deduced for the summer months for a large region around Lake Karakuli, spanning from SW to NE and covering parts of Iran, Central Asia and NW China. During winter, no correlation can be observed directly

CPD
10, 4385–4424, 2014

at the location of the lake, however, precipitation isotopes seem to negatively correlate with precipitation amounts located westwards to our study area (Fig. 6).

In a recent study Tian et al. (2006) found a positive correlation between $\delta^{18}O$ in the local Muztagh Ata ice core (which covers the period 1957–2003) and annual temperatures from Taxkorgan climate station. In contrast they found no significant relationship between ice-core $\delta^{18}O$ and annual precipitation amount at Taxkorgan (Tian et al., 2006). Different precipitation dynamics between middle and high altitudes, and/or seasonal differences, as supported by our LMDZ4-data, could explain this discrepancy. Elevation differences may play a role in different precipitation patterns and these may be associated with isotope effects. The Muztagh Ata glacier accumulation zone receives higher annual precipitation amounts and also a higher proportional input from winter precipitation compared to lower altitudes (Seong et al., 2009a, b). Whilst instrumental and modelling data inferred a slight increase of precipitation amount throughout the last 50 years in the westernmost part of China (Yao et al., 2012; Zhang and Cong, 2014), a decreasing accumulation rate at the Muztagh Ata ice core since 1976 was measured by Duan et al. (2007). Even if the instrumental data from Taxkorgan do not show a significant trend in precipitation amount between 1957 and 2000, this does not rule out changes of snowfall at higher altitudes. Increasing temperatures could have further contributed to the lower observed accumulation rates.

According to the interpretations given above, there are three main factors which potentially influence δD values of biomarkers in our sediment core: (a) temperature, (b) precipitation amount and (c) the proportional uptake of D-depleted source-water in the early vegetation period, which is derived from snow-melt and/or early spring precipitation. Since temperature and precipitation amounts are anti-correlated on an interannual timescale (Fig. 5), we interpret low δD values to indicate both relatively cool and wet conditions. In addition to fluctuations in mean annual precipitation isotopes, snow-melt and delivery to plants may vary. We suggest that a high proportional contribution of water derived from snow-melt, after relatively long and wet winters with high amounts of snowfall, can further lead to more negative δD leaf wax values.

5.3 Paleoclimatic interpretation of downcore data

δD and $\delta^{13}C$ values from Lake Karakuli sediment core suggest relatively warm and dry conditions between ca. 4–3.5 kyr BP (Fig. 7). After that a gradual cooling trend started (interrupted by a warmer/drier period between ca. 3.0 and 2.7 kyr BP), peaking in coolest and wettest conditions around 2.5 kyr BP. Between ca. 2.5 and 1.9 kyr BP a reversal to a slightly warmer and drier climate occurred based on δD evidence. We note that the $\delta^{13}C$ values are rather variable and inconclusive in this core-section, and we observe an offset between δD-C_{26} and δD-C_{28} (these are normally within analytical error of each other). We hypothesize that a warming influenced precipitation isotopes but that the change wasn't intense and stable enough to trigger a large-scale ecosystem response to be recorded in the $\delta^{13}C$ values. Between ca. 1.9 and 1.4 kyr BP, cool and wet conditions occurred again before returning to a warm and dry episode from ca. 1.4 to 0.6 kyr BP (possibly interrupted by a cooling event around 1 kyr BP). The last 0.6 kyr have been mainly cool and wet again, except for the last ca. 100 years, where the topmost three samples of the sediment core indicate another reversal to relatively warm and dry conditions.

Enhanced precipitation, rather than lower temperatures, has been argued to be the main driving force behind growth of glaciers in Asian high-altitude regions (Seong et al., 2009b). The cool/wet episodes deduced from our organic geochemical record match relatively well to reconstructed glacial advances at Mts. Muztagh Ata and Kongur Shan. On basis of ^{10}Be-dating of erratic boulders Seong et al. (2009a) estimated maximal glacial advances at 4.2 ± 0.3, 3.3 ± 0.6, 1.4 ± 0.1 kyr, and a few hundred years before present (Fig. 7). Further, the δD-data are in good agreement with silt-contents in the same sediment core (Fig. 8). These have been interpreted to be influenced by glacial input (Liu et al., 2014) and thus higher contents indicate cooler/wetter conditions.

Our interpretation of lower δD values indicating both relatively cool and wet conditions fits well with results from other late Holocene records in arid Central Asia (Fig. 8). The Little Ice Age (LIA) corresponds to the cool/humid period between 0.6

and 0.1 cal ka BP at Lake Karakuli and has been well documented as a widely humid episode in arid Central Asia (paleoclimatic data compiled in Chen et al., 2010; Fig. 8c). For instance, the Guliya ice core, located ca. 630 km SE from Lake Karakuli, shows relatively high accumulation rates during that period (Fig. 8e), indicating that higher precipitation amounts and not just higher effective moisture (induced by decreased evaporation during cooler conditions) was the main driving force behind e.g. higher lake levels. This very much contrasts the situation in eastern/monsoonal Asia where many records show a relatively dry LIA due to a weakened summer monsoon (Chen et al., 2010 and references therein).

Similarly a number of records have shown a pronounced warm/dry period during the Medieval Climate Anomaly (MCA; Fig. 8c and e; Chen et al., 2010; Lauterbach et al., 2014; Esper et al., 2002) also seen in our record from Late Karakuli. At ca. 1 cal ka BP we observe a ca. 100 year interruption of this event indicated by three samples with lower δD values. Recently, Lei et al. (2014) observed a similar spike in carbonate $\delta^{18}O$ values from Lake Sasi Kul, which is located ca. 190 km west of our study site (Fig. 8b). Thus we hypothesize that this interruption was not just a local phenomenon. Warm and dry conditions during the MCA have also been observed at Kashgar (western Tarim Basin; just ca. 150 km north of Lake Karakuli; Zhao et al., 2012), and from from Lakes Bangong Co on the western Tibetan Plateau (Gasse et al., 1996) and large Karakul in the Tajik Pamir (Mischke et al., 2010).

Applying these findings to the complete record we see fluctuating climatic conditions throughout the late Holocene with clearly identifiable warmer/drier and cooler/wetter episodes (Fig. 8). During the oldest section of our record (ca. 4.2–3.4 kyr BP) average conditions appeared having been warmer and drier than during the medieval and today, followed by a general (even though non-continuous) cooling trend until ca. 2.4 kyr BP. A cool and wet phase of roughly 1000 years starting at ca. 3.5 kyr BP has been observed in numerous global climate records (Mayewski et al., 2004). At the nearby oasis of Kashgar, conditions prevailed relatively wet from ca. 4.0 until ca. 2.6 kyr BP (Zhao et al., 2012). At the large Lake Karakul in Tajikistan a rapid drop

CPD
10, 4385–4424, 2014

of TOC-contents occurred at ca. 3.5 cal ka BP, indicating a drop of lake productivity probably induced by low-temperatures and eventually associated with shorter ice-free periods in the summer (Mischke et al., 2010; Fig. 8g). At Lake Balikun (northeastern Xinjiang) a reversal to wetter conditions occurred after a pronounced dry event lasting from 4.3–3.8 kyr BP (An et al., 2012). In Lake Manas (northern Xinjiang) a wet episode was reconstructed for 4.5–2.5 kyr BP, interrupted by a short dry period between 3.8–3.5 kyr BP (Rhodes et al., 1996). Low δ^{18}O values in the Guliya ice core between 3.5 and 3.0 kyr BP also give evidence for low temperatures on the northwestern Tibetan Plateau (Thompson et al., 1997) while in the southern Tarim Basin a rapid shift to wetter conditions at ca. 3.0 kyr BP have been observed (Zhong et al., 2007).

After a ca. 500 year slight warming (ca. 2.4–1.9 kyr BP; synchronous with the Roman Warm Period; RWP), another reversal into cool and wet condition occurred, peaking at ca. 1.8–1.6 kyr BP (often referred to as Dark Ages Cool Period, DACP, or Migration Period). Both of these events have also been observed in the nearby Kashgar (Zhao et al., 2012). Afterwards that the climatic trend gradually transitioned into the above mentioned warm period during the medieval, followed by the LIA and the current warming period (CWP), the latter indicated by increased δD values in the topmost three samples of the sediment core.

5.4 Implications for Central Asian climate dynamics

The sequence of relatively cool/wet and warm/dry episodes displays coherency with other records of Northern Hemisphere climate records. There is a similarity between cyclicity of cooling events at Lake Karakuli, Northern Atlantic ice-rafting events (Fig. 8i; Bond et al., 2001) and strengthening phases of the Siberian High (the anticyclonic high pressure ridge over Siberia), the latter recorded by [K^+] increases in the GISP2 ice core between ca. 3.5–2.8 and 0.5–0.2 kyr BP (Fig. 8h; Mayewski et al., 1997). Further, throughout the last ca. 1000 years, δD values of leaf waxes in Lake Karakuli are correlated with the mode of the North Atlantic Oscillation (NAO), showing more positive

CPD
10, 4385–4424, 2014

values during the current and medieval positive mode and more negative values during the LIA-negative mode (Fig. 8f; Trouet et al., 2009).

The interplay between the dominant atmospheric circulation systems in Central Asia – the Siberian High, the mid-latitude Westerlies and partly the Indian Summer Monsoon – as well as orographic influences, lead to complex climatic patterns. Trajectory studies in the modern atmosphere, as well as inventories of dust particles in ice cores, suggest the mid-latitude Westerlies as primary source of moisture during winter and spring, with the North Atlantic, the Mediterranean, the Black and Caspian Sea as possible regions of origin (Lei et al., 2014; Seong et al., 2009a, b; Wu et al., 2008). The Siberian High delivers cool but also relatively dry air during winter. The absence of sea-salt i.e. in the Muztagh Ata ice core (Aizen et al., 2001; Seong et al., 2009b) further gives evidence for a minor importance of the Indian Monsoon, and for mid-latitude Westerlies and local convection to be the most important moisture sources during the summer.

Even though Lake Karakuli receives some moisture in spring (Fig. 4), regions which are located as close as 190 km westwards at a similar altitude, such as Lake Sasi Kul and other parts of the central and western Pamirs receive much higher proportions and amounts of winter and spring precipitation (Lei et al., 2014; Miehe et al., 2001). Variations of strength and tracks of the Westerlies and related movement of the Polar Front (Machalett et al., 2008) could have influenced the amount of winter and spring moisture which has reached the Karakuli-region in the past. Lei et al. (2014) suggested that during negative NAO-modes (e.g. during the LIA) the storm tracks were moving further southwards, leading to wetter conditions in the Mediterranean and higher amounts of moisture been transported into Central Asian realms of the same latitude. In contrast other authors proposed a more complex interplay between the Eurasian and Pacific circulation systems on basis of modelling data, and a generally higher delivery of moisture into Central Asia during episodes of strengthened Westerlies (i.e. positive NAO-modes) (Syed et al., 2010; Syed, 2011). Recently, a possible negative correlation between lower winter precipitation in the Mediterranean (positive NAO-mode) and higher winter precipitation at Son Kol (central Tien Shan; ca. 400 km north

CPD
10, 4385–4424, 2014

of Lake Karakuli) was also suggested by Lauterbach et al. (2014) on basis of δ^{15}N-data on total nitrogen (Fig. 8d).

Based on our data, we hypothesize that the relatively wet episodes recorded in our sediment core from Lake Karakuli were mainly caused by increased late-winter and spring precipitation derived from mid-latitude Westerlies. Cooling/wettening periods at 3.5 cal ka BP and between 1.9 and 1.5 kyr BP (DACP) are simultaneous with increased winter precipitation at Son Kol (Fig. 8d), indicating common climatic variations in the eastern Pamirs and the central Tien Shan. For the LIA, this connection is less pronounced. Instead, for the last ca. 1.5 kyr BP, we see a close similarity to isotopic trends in the central Pamirs (Fig. 8b), which in turn drift apart between 1.5 and 2.5 kyr BP. An explanation for this could be the increased influence of the significantly strengthened Siberian High during the LIA (Fig. 8h). This possibly weakened the mid-latitude Westerlies or pushed their tracks further to the south, resulting in comparably drier conditions at more northern regions such as the Tien Shan, but wetter conditions in the central and eastern Pamirs (Lei et al., 2014). A similar mechanism could explain the climatic pattern in the eastern Pamirs at present, with low winter and spring precipitation at low altitudes during the current positive NAO-mode and Westerlies penetrating more to the North, while the central Pamirs still receive high winter precipitation.

Despite a slight increase in total precipitation amount over the last 50 years in the dry areas of Western China (Zhang and Cong, 2014), effective moisture has decreased due to rising temperatures. The two closed ponds and Lake Karakuli itself, show clear geomorphological evidence for recent shrinking (field observations) and isotopic evidence for evaporative enrichment above meteoric waters (Table 1). This is in contrast to several endorheic lakes in Central Asia, whose lake levels are rising due to the currently increased meltwater input from receding glaciers (e.g. Bosten Lake; Wünnemann et al., 2006; or large Lake Karakul, Mischke et al., 2010).

CPD
10, 4385–4424, 2014

6 Conclusions

The biomarker isotopic record of Lake Karakuli, eastern Pamirs, shows distinct episodes of relatively cool/wet and warm/dry climate over the last 4200 years. We find cool/wet episodes in the region coincide with North Atlantic ice rafting events and periods of strengthening of the Siberian High. However there are also indications for complex responses of regional climate, i.e. different responses between the western (e.g. Western and Central Pamir), eastern (e.g. Eastern Pamir) and northern (e.g. Tien Shan) parts of Central Asia. We suggest that these differences arise from changes in the extent and pathways of the Westerlies. Our data provide evidence that the transition between regions of summer-only and winter/spring dominated precipitation could have been a key factor for local climate in the past. We further show a rapid aridification in the eastern Pamir during the last 50–100 years.

The Supplement related to this article is available online at doi:10.5194/cpd-10-4385-2014-supplement.

Acknowledgements. This work was supported by the German Academic Exchange Service (DAAD) postdoctoral fellowship to B. Aichner at the University of Southern California (USC) and by USC to S. Feakins for analytical costs. Funding from the DFG supported the fieldwork. We thank Hanno Meyer and Lutz Schoenicke (AWI Potsdam) for providing isotopic data of water samples. We are further grateful for help during field work (Jian Ni and Yang Bo), for assistance with core sampling (Yongbo Wang) and for analytical support at USC (Miguel Rincon).

References

Aichner, B., Herzschuh, U., and Wilkes, H.: Influence of aquatic macrophytes on stable carbon isotope signatures of sedimentary organic matter in lakes on the Tibetan Plateau, Org. Geochem., 41, 706–718, 2010a.

CPD
10, 4385–4424, 2014

Aichner, B., Herzschuh, U., Wilkes, H., Mischke, S., and Zhang, C.: Biomarker and compound-specific carbon isotope evidence for changing environmental and carbon-limiting conditions at Koucha Lake, Eastern Tibetan Plateau, J. Paleolimnol., 43, 873–899, 2010b.

Aichner, B., Herzschuh, U., Wilkes, H., Vieth, A., and Böhner, J.: δD values of *n*-alkanes in Tibetan lake sediments and aquatic macrophytes a surface sediment study and application to a 16 ka record from Lake Koucha, Org. Geochem., 41, 779–790, 2010c.

Aizen, E. M., Aizen, V. B., Melack, J. M., Nakamura, T., and Ohta, T.: Precipitation and atmospheric circulation patterns at mid-latitudes of Asia, Int. J. Climatol., 21, 535–556, 2001.

Allen, E. D. and Spence, D. H. N.: The differential ability of aquatic plants to utilize the inorganic carbon supply in fresh water, New Phytol., 87, 269–283, 1981.

An, C. B., Feng, Z. D., and Barton, L.: Dry or humid?, Mid-Holocene humidity changes in arid and semi-arid China, Quaternary Sci. Rev., 25, 351–361, 2006.

An, C. B., Lu, Y., Zhao, J., Tao, S., Dong, W., Li, H., Jin, M., and Wang, Z.: A high-resolution record of Holocene environmental and climatic changes from Lake Balikun (Xinjiang, China): implications for central Asia, Holocene, 22, 43–52, 2012.

Araguás-Araguás, L., Froehlich, K., and Rozanski, K.: Stable isotope composition of precipitation over southeast Asia, J. Geophys. Res.-Atmos., 103, 28721–28742, 1998.

Blaauw, M. and Christen, J. A.: Flexible paleoclimate age-depth models using an autoregressive gamma process, Bayesian Anal., 6, 457–474, 2011.

Bond, G., Kromer, B., Beer, J., Muscheler, R., Evans, M., Showers, W., Hoffmann, S., Lotti-Bond, R., Hajdas, I., and Bonani, G.: Persistent solar influence on North Atlantic climate during the Holocene, Science, 294, 2130–2136, 2001.

Boomer, I., Wünnemann, B., Mackay, A. W., Austin, P., Sorrell, P., Reinhardt, C., Keyser, C., Guichard, F., and Fontugne. M.: Advances in understanding the late Holocene history of the Aral Sea region, Quatern. Int., 194, 79–90, 2009.

Bowen, G. J. and Revenaugh, J.: Interpolating the isotopic composition of modern meteoric precipitation, Water Resour. Res., 39, 1299–1311, 2003.

Chen, F. H., Yu, Z. C., Yang, M. L., Ito, E., Wang, S., Madsen, D. B., Huang, X., Zhao, Y., Sato, T., Birks, J. B., Boomer, I., Chen, J., An, C., and Wünnemann, B.: Holocene moisture evolution in arid central Asia and its out-of-phase relationship with Asian monsoon history, Quaternary Sci. Rev., 27, 351–364, 2008.

Chen, F. H., Chen, J. H., Holmes, J. A., Boomer, I., Austin, P., Gates, J. B., Wang, N. L., Brooks, S. J., and Zhang, J. W.: Moisture changes over the last millennium in the arid central

Asia: a review, synthesis and comparison with monsoon region, Quaternary Sci. Rev., 29, 1055–1068, 2010.

Cheng. H., Zhang, P. Z., Spötl, C., Edwards, R. L., Cai, Y. J., Zhang, D. Z., Sang, W. C., Tan, M., and An, Z. S.: The climatic cyclicity in semiarid-arid central Asia over the past 500,000 years, Geophys. Res. Lett., 39, L01705, doi:10.1029/2011GL050202, 2012.

Chikaraishi, Y. and Naraoka, H.: δ^{13}C and δD identification of sources of lipid biomarkers in sediments of Lake Haruna (Japan), Geochim. Cosmochim. Ac., 69, 3285–3297, 2005.

Dansgaard, W.: Stable isotopes in precipitation, Tellus, 16, 436–468, 1964.

Duan, K., Yao, T., Wang, N. L., Tian, L. D., Xu, B. Q., and Wu, G. J.: Records of precipitation in the Muztag Ata ice core and its climate significance to glacier water resources, J. Glaciol. Geocryol., 29, 680–684, 2007.

Esper, J., Schweingruber, F. H., and Winiger, M.: 1300 years of climatic history for western Central Asia inferred from tree-rings, Holocene, 12, 267–277, 2002.

Fan, L. L., Tang., L. S., Wu, L. F., Ma., J., and Li, Y.: The limited role of snow water in the growth and development of ephemeral plants in a cold desert, J. Veg. Sci., 25, 681–690, 2014.

Feakins, S. J. and Sessions, A. L.: Controls on the D / H ratios of plant leaf waxes from an arid ecosystem, Geochim. Cosmochim. Ac., 74, 2128–2141, 2010.

Feakins, S. J., Kirby, M. E., Cheetham, M. I., Ibarra, Y., and Zimmerman, S. R. H.: Fluctuation in leaf wax D/H ratio from a southern California lake records significant variability in isotopes in precipitation during the late Holocene, Org. Geochem., 66, 48–59, 2014.

Ficken, K. J., Li, B., Swain, D. L., and Eglinton, G.: An *n*-alkane proxy for the sedimentary input of submerged/floating freshwater aquatic macrophytes, Org. Geochem., 31, 745–749, 2000.

Gasse, F., Fontes, J. C., VanCampo, E., and Wei, K.: Holocene environmental changes in Bangong Co basin (western Tibet), 4. Discussion and conclusions, Palaeogeogr. Palaeocl., 120, 79–92, 1996.

Gat, J. R.: Oxygen and hydrogen isotopes in the hydrologic cycle, Annu. Rev. Earth Pl. Sc., 24, 225–262, 1996.

Günther, F., Aichner, B., Siegwolf, R., Xu, B. Q., Yao, T., and Gleixner, G.: A synthesis of hydrogen isotope variability and its hydrological significance at the Qinghai-Tibetan Plateau, Quatern. Int., 313–314, 3–16, 2013.

Herzschuh, U.: Paleo-moisture evolution in monsoonal Central Asia during the last 50,000 years, Quaternary Sci. Rev., 25, 163–178, 2006.

Hourdin, F., Musat, I., Bony, S., Braconnot, P., Codron. F., Dufresne, J. L., Fairhead, L., Filiberti, M. A., Friedlingstein, P., Grandpeix, J. Y., Krinner, G., LeVan, P., Li, Z. X., and Lott, F.: The LMDZ4 general circulation model: climate performance and sensitivity to parametrized physics with emphasis on tropical convection, Clim. Dynam., 27, 787–813, 2006.

Huang, X., Oberhänsli, H., von Suchodoletz, H., and Sorrell, P.: Dust deposition in the Aral Sea: implications for changes in atmospheric circulation in central Asia during the past 2000 years, Quaternary Sci. Rev., 30, 3661–3674, 2011.

Kahmen, A., Hoffmann, B., Schefuß, E., Arndt, S. K., Cernusak, L. A., West, J. B., and Sachse, D.: Leaf water deuterium enrichment shapes leaf wax *n*-alkane δD values of angiosperm plants II: observational evidence and global implications, Geochim. Cosmochim. Ac., 111, 50–63, 2013a.

Kahmen, A., Schefuss, E., and Sachse, D.: Leaf water deuterium enrichment shapes leaf wax *n*-alkane δD values of angiosperm plants I: experimental evidence and mechanistic insights, Geochim. Cosmochim. Ac., 111, 39–49, 2013b.

Kusch, S., Rethemeyer, J., Schefuß, E., and Mollenhauer, G.: Controls on the age of vascular plant biomarkers in Black Sea sediments, Geochim. Cosmochim. Ac., 74, 7031–7047, 2010.

Lauterbach, S., Witt., R., Plessen., B., Dulski, P., Prasad, S., Mingram, J., Gleixner, G., Hettler-Riedel., S., Stebich, M., Schnetger, B., Schwalb, A., and Schwarz. A.: Climatic imprint of the mid-latitude Westerlies in the Central Tian Shan of Kyrgyzstan and teleconnections to North Atlantic climate variability during the last 6000 years, Holocene, 24, 970–998, 2014

Lee, J.-E. and Fung, I.: “Amount effect” of water isotopes and quantitative analysis of post-condensation processes, Hydrol. Process., 22, 1–8, 2008.

Lee, J. E., Risi, C., Fung, I., Worden, J., Scheepmaker, R. A., Lintner, B., and Frankenberg, C.: Asian monsoon hydrometeorology from TES and SCIAMACHY water vapor isotope measurements and LMDZ simulations: implications for speleothem climate record interpretation, J. Geophys. Res., 117, D15112, doi:10.1029/2011JD017133, 2012.

Lei, Y., Tian, L. D., Bird, B. W., Hou, J., Ding, L., Oimahmadov, I., and Gadoev, M.: A 2540 year record of moisture variations derived from lacustrine sediment (Sasikul Lake) on the Pamir Plateau, Holocene, 24, 761–777, 2014.

Liu, X., Herzschuh, U., Shen, J., Jiang, Q., and Xiao, X.: Holocene environmental and climatic changes inferred from Wulungu Lake in northern Xinjiang, China, Quaternary Res., 70, 412–425, 2008.

CPD
10, 4385–4424, 2014

Liu, X., Herzschuh, U., Wang, Y., Kuhn, G., and Yu, Z.: Glacier fluctuations of Muztagh Ata and temperature changes during the late Holocene in westernmost Tibetan Plateau, based on glaciolacustrine sediment records, Geophys. Res. Lett., 41, 6265–6273, 2014.

Liu, Z. H., Henderson, A. C. G., and Huang, Y. S.: Regional moisture source changes inferred from Late Holocene stable isotope records, Adv. Atmos. Sci., 25, 1021–1028, 2008.

Machalett, B., Oches, E. A., Frechen, M., Zöller, L., Hambach, U., Mavlyanova, N. G., Markoviæ, S. B., and Endlicher, W.: Aeolian dust dynamics in central Asia during the Pleistocene: driven by the long-term migration, seasonality, and permanency of the Asiatic polar front, Geochem. Geophy. Geosy., 9, Q08Q09, doi:10.1029/2007GC001938, 2008.

Mathis, M., Sorrel, P., Klotz, S., Huang, X., and Oberhänsli, H.: Regional vegetation patterns at lake Son Kul reveal Holocene climatic variability in central Tien Shan (Kyrgyzstan, Central Asia), Quaternary Sci. Rev., 89, 169–185, 2014.

Mayewski, P. A., Meeker, L. D., Twickler, M. S., Whitlow, S., Yang, Q., Lyons, W. B., and Prentice, M.: Major features and forcing of high-latitude Northern Hemisphere atmospheric circulation using a 110,000-year-long glaciochemical series, J. Geophys. Res., 102, 26345–26366, 1997.

Mayewski, P. A., Rohling, E. E., Stager, J. C., Karlén, W., Maasch, K. A., Meeker, L. D., Meyerson, E. A., Gasse, F., van Kreveld, S., Holmgren, K., Lee-Thorp, J., Rosqvist, G., Rack, F., Staubwasser, M., Schneider, R. R., and Steig, E. J.: Holocene climate variability, Quaternary Res., 62, 243–255, 2004.

Miehe, G., Winiger, M., Böhner, J., and Yili, Z.: Climatic diagram map of high Asia, purpose and concepts, Erdkunde, 55, 94–97, 2001.

Mischke, S., Rajabov, I., Mustaeva, N., Zhang, C. J., Boomer, I., Brown, E. T., Andersen, N., Myrbo, A., Ito, E., and Schudack, M. E.: Modern hydrology and late Holocene history of Lake Karakul, eastern Pamirs (Tajikistan): a reconnaissance study, Palaeogeogr. Palaeocl., 289, 10–24, 2010.

Morill, C., Overpeck, J. T., and Cole, J. E.: A synthesis of abrupt changes in the Asian summer monsoon since the last deglaciation, Holocene, 13, 465–476, 2003.

Mügler, I., Gleixner, G., Günther, F., Mäusbacher, R., Daut, G., Schütt, B., Berking, J., Schwalb, A., Schwark, L., Xu, B., Yao, T., Zhu, L., and Yi, C.: A multi-proxy approach to reconstruct hydrological changes and Holocene climate development of Nam Co, Central Tibet, J. Paleolimnol., 43, 625–648, 2010.

CPD
10, 4385–4424, 2014

Narama, C.: Late Holocene variation of the raigorodskogo glacier and climate change in the Pamir-Alai, central Asia, Catena, 48, 21–37, 2002a.
Narama, C.: Glacier variations in Central Asia during the 20th century, J. Geogr., 111, 486–497, 2002b.
Prins, H. B. A. and Elzenga, J. T. M.: Bicarbonate utilization: function and mechanism, Aquat. Bot., 34, 59–83, 1989.
Rach, O., Brauer, A., Wilkes, H., and Sachse, D.: Delayed hydrological response to Greenland cooling at the onset of the Younger Dryas in western Europe, Nat. Geosci., 7, 109–112, doi:10.1038/ngeo2053, 2014.
Rayner, N. A., Parker, D. E., Horton, E. B., Folland, C. K., Alexander, L. V., Rowell, D. P., Kent, E. C., and Kaplan, A.: Global analyses of sea surface temperature, sea ice, and night marine air temperature since the late nineteenth century, J. Geophys. Res., 108, 4407, doi:10.1029/2002JD002670, 2003.
Reimer, P. J., Baillie, M. G. L., Bard, E., Bayliss, A., Beck, J. W., Blackwell, P. G., Ramsey, C. B., Buck, C. E., Burr, G. S., and Edwards, R. L. E.: IntCal09 and Marine09 radiocarbon age calibration curves, 0–50,000 years cal BP, Radiocarbon, 51, 1111–1150, 2009.
Rhodes, T. E., Gasse, F., Lin, R., Fontes, J. C., Wei, K., Bertrand, P., Gilbert, E., Mélières, F., Tucholka, P., and Cheng, Z. Y.: A late pleistocene-Holocene lacustrine record from Lake Manas, Zunggar (northern Xinjiang, western China), Palaeogeogr. Palaeocl., 120, 105–121, 1996.
Ricketts, R. D., Johnson, T. C., Brown, E. T., Rasmussen, K. A., and Romanovsky, V. V.: Holocene, paleolimnology of Lake Issyk-Kul, Kyrgyzstan: trace element and stable isotope composition of ostracodes, Palaeogeogr. Palaeocl., 176, 207–227, 2001.
Risi, C., Bony, S., Vimeux, F., and Jouzel, J.: Water-stable isotopes in the LMDZ4 general circulation model: model evaluation for present-day and past climates and applications to climatic interpretations of tropical isotopic records, J. Geophys. Res., 115, D12118, doi:10.1029/2009JD013255, 2010.
Risi, C., Noone, D., Worden, J., Frankenberg, C., Stiller, G., Kiefer, M., Funke, B., Walker, K., Bernath, P., Schneider, M., Wunch, D., Sherlock, V., Deutscher, N., Griffith, D., Wennberg, P. O., Strong, K., Smale, D., Mahieu, E., Barthlott, S., Hase, F., García, O., Notholt, J., Wameke, T., Toon, G., Sayres, D., Bony, S., Lee, J., Brown, D., Uemura, R., and Sturm, C.: Process-evaluation of tropospheric humidity simulated by general

circulationmodels using water vapor isotopologues: 1. Comparison between models and observations, J. Geophys. Res., 117, D05303, doi:10.1029/2011JD016621, 2012a.
Risi, C., Noone, D., Worden, J., Frankenberg, C., Stiller, G., Kiefer, M., Funke, B., Walker, K., Bernath, P., Schneider, M., Bony, S., Lee, J., Brown, D., and Sturm, C.: Process-evaluation of tropospheric humidity simulated by general circulation models using water vapor isotopic observations: 2. Using isotopic diagnostics to understand the mid and upper tropospheric moist bias in the tropics and subtropics, J. Geophys. Res., 117, D05304, doi:10.1029/2011JD016623, 2012b.
Sachse, D., Billault, I., Bowen, G. J., Chikaraishi, Y., Dawson, T. E., Feakins, S. J., Freeman, K. H., Magill, C. R., McInerney, F. A., van der Meer, M. T. J., Polissar, P., Robins, R. J., Sachs, J. P., Schmidt, H.-L., Sessions, A. L., White, J. W. C., West, J. B., and Kahmen, A.: Molecular paleohydrology: interpreting the hydrogen-isotopic composition of lipid biomarkers from photosynthesizing organisms, Annu. Rev. Earth Pl. Sc., 40, 221–249, 2012.
Schefuss, E., Schouten, S., and Schneider, R.: Climatic controls on central African hydrology during the past 20,000 years, Nature, 473, 1003–1006, 2005.
Seong, Y. B., Owen, L. A., Yi, C., and Finkel, R. C.: Quaternary glaciation of Muztag Ata and Kongur Shan: evidence for glacier response to rapid climate changes throughout the Late Glacial and Holocene in westernmost Tibet, Geol. Soc. Am. Bull., 121, 348–365, 2009a.
Seong, Y. B., Owen, L. A., Yi, C. L., Finkel, R. C., and Schoehnbohm, L.: Geomorphology of anomalously high glaciated mountains at the northwestern end of Tibet: Muztag Ata and Kongur Shan, Geomorphology, 103, 227–250, 2009b.
Sessions, A. L., Burgoyne, T. W., and Hayes, J. M.: Correction of H_3 contributions in hydrogen isotope ratio monitoring mass spectrometry, Anal. Chem., 73, 192–199, 2001.
Seth, A., Rauscher, S. A., Rojas., M., Giannini, A., and Camargo, S. J.: Enhanced spring convective barrier for monsoons in a warmer world?, a letter, Climatic Change, 104, 403–414, 2011.
Smith, F. A. and Freeman, K. H.: Influence of physiology and climate on δD of leaf wax *n*-alkanes from C_3 and C_4-grasses, Geochim. Cosmochim. Ac., 70, 1172–1187, 2006.
Sorrel, P., Popescu, S. M., Klotz, S., Suc, J. P., and Oberhänsli, H.: Climate variability in the Aral Sea basin (Central Asia) during the late Holocene based on vegetation changes, Quaternary Res., 67, 357–370, 2007a.

CPD
10, 4385–4424, 2014

Sorrel, P., Oberhänsli, H., Boroffka, N., Nourgaliev, D., Dulski, P., and Röhl, U.: Control of wind strength and frequency in the Aral Sea basin during the late Holocene, Quaternary Res., 67, 371–382, 2007b.

Syed, F. S.: On the Intra-Seasonal to Decadal Climate Variability Over South-Asia, Dissertation, Department of Meteorology, Stockholm University, Sweden, 2011.

Syed, F. S., Giorgi, F., Pal, J. S., and Keay, K.: Regional climate model simulation of winter climate over Central-Southwest Asia, with emphasis on NAO and ENSO effects, Int. J. Climatol., 30, 220–235, 2010.

Thompson, L. G.: Ice core evidence for climate change in the Tropics: implications for our future, Quaternary Sci. Rev., 19, 19–35, 2000.

Thompson, L. G., Yao, T., Davis, M. E., Henderson, K. A., Mosley-Thompson, E., Lin, P.-N., Beer, J., Synal, H. A., Cole-Dai, J., and Bolzan, J. F.: Tropical climate instability: the last glacial cycle from a Qinghai-Tibetan ice core, Science, 276, 1821–1825, 1997.

Tian, L., Yao, T., Li, Z., MacClune, K., Wu, G., Xu, B., Li, Y., Lu, A., and Shen, Y.: Recent rapid warming trend revealed from the isotopic record in Muztagata ice core, eastern Pamirs, J. Geophys. Res., 111, D13103, doi:10.1029/2005JD006249, 2006.

Tierney, J. E., Russell, J. M., Huang, Y. S., Sinninghe Damsté, J. S., Hopmans, E. C., and Cohen, A. S.: Northern Hemisphere controls on tropical southeast African climate during the past 60,000 years, Science, 322, 252–255, 2008.

Treydte, K. S., Schleser, G. H., Helle, G., Frank, D. C., Winiger, M, Haug, G., and Esper, J.: The twentieth century was the wettest period in northern Pakistan over the past millennium, Nature, 440, 1179–1182, 2006.

Trouet, V., Esper, J., Graham, N. E., Baker, A., Scourse, J. D., and Frank, D. C.: Persistent positive North Atlantic Oscillation mode dominated the Medieval Climate Anomaly, Science, 324, 78–80, 2009.

Uppala, S. M., KÅllberg, P. W., Simmons, A. J., Andrae, U., Bechtold, V. D. C., Fiorino, M., Gibson, J. K., Haseler, J., Hernandez, A., Kelly, G. A., Li, X., Onogi, K., Saarinen, S., Sokka, N., Allan, R. P., Andersson, E., Arpe, K., Balmaseda, M. A., Beljaars, A. C. M., Berg, L. V. D., Bidlot, J., Bormann, N., Caires, S., Chevallier, F., Dethof, A., Dragosavac, M., Fisher, M., Fuentes, M., Hagemann, S., Hólm, E., Hoskins, B. J., Isaksen, L., Janssen, P. A. E. M., Jenne, R., Mcnally, A. P., Mahfouf, J.-F., Morcrette, J.-J., Rayner, N. A., Saunders, R. W., Simon, P., Sterl, A., Trenberth, K. E., Untch, A., Vasiljevic, D., Viterbo, P., and Woollen, J.: The ERA-40 re-analysis, Q. J. Roy. Meteor. Soc., 131, 2961–3012, 2005.

CPD
10, 4385–4424, 2014

Wang, Z. and Liu, W.: Carbon chain length distribution in *n*-alkyl lipids: a process for evaluating source inputs to Lake Qinghai, Org. Geochem., 50, 36–43, 2012.
Wu, G. J., Yao, T. D., Xu, B. Q., Tian, L. D., Li, Z., and Duan, K. Q.: Seasonal variations of dust record in the Muztagata ice cores, Chinese Sci. Bull., 53, 2506–2512, 2008.
Wünnemann, B., Mischke, S., and Chen, F.: A Holocene sedimentary record from Bosten Lake, China, Palaeogeogr. Palaeocl., 234, 223–238, 2006.
Wünnemann, B., Demske, D., Tarasov, P., Kotlia, B. S., Reinhardt, C., Bloemendal, J., Diekmann, B., Hartmann, K., Krois, J., Riedel, F., and Arya, N.: Hydrological evolution during the last 15 kyr in the Tso Kar lake basin (Ladakh, India), derived from geomorphological, sedimentological and palynological records, Quaternary Sci. Rev., 29, 1138–1155, 2010.
Yao, T., Thompson, L., Yang, W., Yu, W., Gao, Y., Guo, X., Yang, X., Duan, K., Zhao, H., Xu, B., Pu, J., Lu, A., Xiang, Y., Kattel, D. B., and Joswiak, D.: Different glacier status with atmospheric circulations in Tibetan Plateau and surroundings, Nat. Clim. Change, 2, 663–667, 2012.
Yao, T., Masson-Delmotte, V., Gao, J., Yu, W., Yang, X., Risi, C., Sturm, C., Werner, M., Zhao, H., He, Y., Ren, W., Tian, L., Shi, C., and Hou, S.: A review of climatic controls on $\delta^{18}O$ in precipitation over the Tibetan Plateau: observations and simulations, Rev. Geophys., 51, 525–548, 2013.
Zhang, X. and Cong, Z.: Trends of precipitation intensity and frequency in hydrological regions of China from 1956 to 2005, Global Planet. Change, 117, 40–51, 2014
Zhao, K., Li, X., Dodson, J., Atahan, P., Zhou, X., and Bertuch, F.: Climatic variations over the last 4000 cal yr BP in the western margin of the Tarim Basin, Xinjiang, reconstructed from pollen data, Palaeogeogr. Palaeocl., 321, 16–23, 2012.
Zhong, W., Xue, J. B., Shu, Q., and Wang, L. G.: Climatic change during the last 4000 years in the southern Tarim Basin, Xinjiang, northwest China, J. Quaternary Sci., 22, 659–665, 2007.

CPD
10, 4385–4424, 2014

Late Holocene paleoclimate in arid Central Asia

B. Aichner et al.

Table 1. $\delta^{18}O$ and δD values of water samples collected in September 2008 at Lake Karakuli, its inflows and nearby ponds.

Latitude [° N]	Longitude [° E]	Altitude [m]	Description	$\delta^{18}O$	1σ [‰]	δD [‰]	1σ
38.41933	75.05995	3684	inflow1	−12.1	0.05	−83.2	0.2
38.42021	75.05008	3688	inflow2	−12.1	0.01	−84.4	0.2
38.43968	75.05725	3657	Karakuli – core position surface water	−9.4	0.04	−67.8	0.2
38.43968	75.05725	3657	Karakuli – core position above sediment	−9.2	0.03	−67.2	0.2
38.46294	75.02944	3658	small pond near Karakuli	5.45	0.02	13.5	0.4
38.46314	75.04267	3676	larger pond near Karakuli	−3.6	0.02	−37.1	0.5

CPD
10, 4385–4424, 2014

Late Holocene paleoclimate in arid Central Asia

B. Aichner et al.

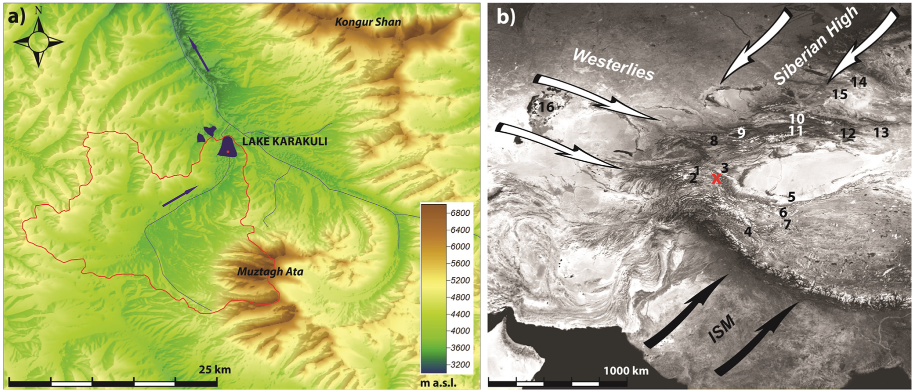

Figure 1. (a) Catchment of Lake Karakuli and coring position (red dot). **(b)** Location of our study area (red cross) and other paleoclimatic records mentioned in the text. 1: large Lake Karakul, Tajikistan (Mischke et al., 2010); 2: Lake Sasi Kul (Lei et al., 2014); 3: Kashgar (Zhao et al., 2012); 4: Tso Kar (Wünnemann et al., 2010); 5: Southern Tarim Basin (Zhong et al., 2007); 6: Guliya Ice Core (e.g. Thompson et al., 1997); 7: Lake Bangong (Gasse et al., 1996); 8: Son Kol (Lauterbach et al., 2014; Mathis et al., 2014), 9: Issyk Kul (Ricketts et al., 2001); 10: Yili section (Li et al., 2011); 11: Kesang Cave (Cheng et al., 2012); 12: Boston Hu (Wünnemann et al., 2006); 13: Lake Balinkun (An et al., 2012); 14: Ulungur Hu (Liu et al., 2008); 15: Lake Manas (Rhodes et al., 1996); 16: Aral Sea (Sorrell et al., 2007a, b; Boomer et al., 2009; Huang et al., 2011).

CPD
10, 4385–4424, 2014

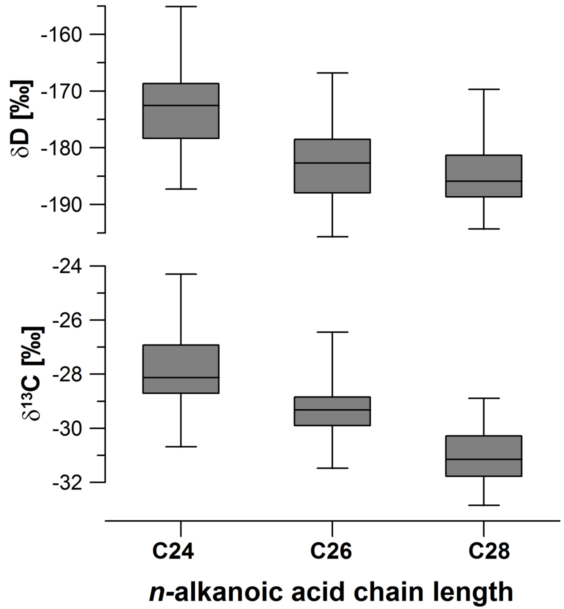

Figure 2. Box and whisker plots of δD and δ^{13}C values in sediment samples by chain length.

CPD
10, 4385–4424, 2014

Title Page
Abstract | Introduction
Conclusions | References
Tables | Figures
◂ | ▸
Back | Close
Full Screen / Esc
Printer-friendly Version
Interactive Discussion

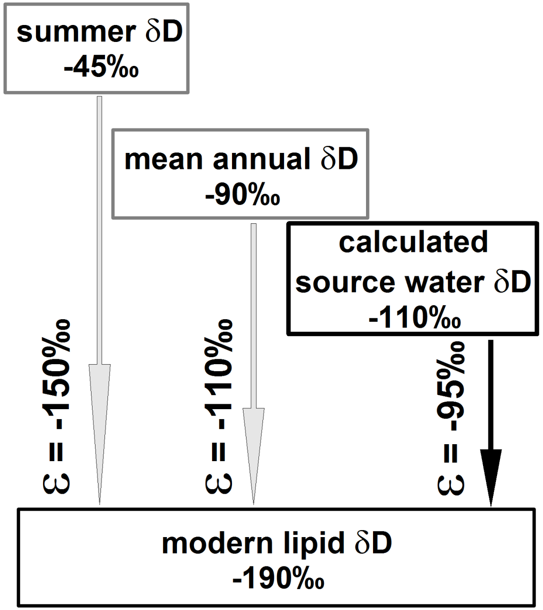

Figure 3. Calculated isotopic fractionation factors (ε) between summer and mean annual precipitation and modern lipids, as well as calculated source water δD on basis of published fractionation factors in arid ecosystems (ca. −95 ‰ according to Feakins and Sessions, 2010; Günther et al., 2013).

CPD
10, 4385–4424, 2014

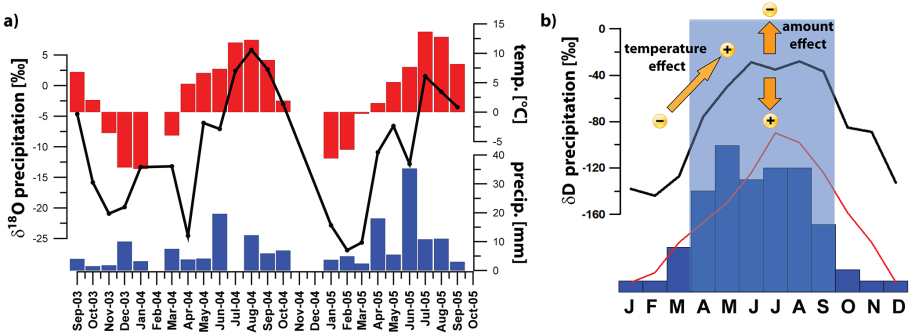

Figure 4. (a) Monthly isotopic and climate data from Taxkorgan climate station (Yao et al., 2013), located ca. 80 km south of Lake Karakuli (altitude ca. 3100 m). **(b)** Average monthly climate (Miehe et al., 2001) and isotopic (OIPC; Bowen and Revenaugh, 2003) data from Bulun Kol climate station located ca. 30 km northeast of Lake Karakuli (altitude ca. 3300 m). Shaded area indicates summer/wet season.

CPD
10, 4385–4424, 2014

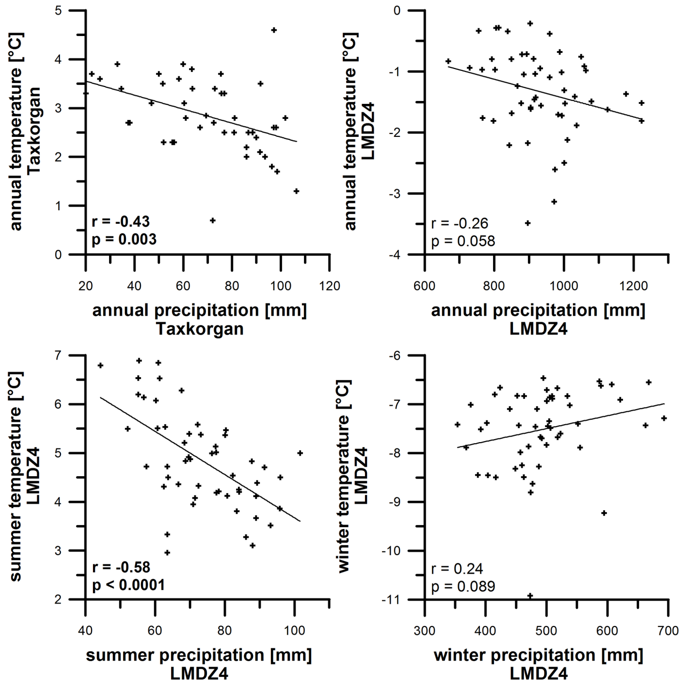

Figure 5. Correlations of temperatures with precipitation amounts based on instrumental data from Taxkorgan meteorological station (1957–2000; annual averages) and model data using LMDZ4 simulations (1958–2009; summer: April–September; winter: October–March). Bold correlation coefficients are significant at the 0.01-level.

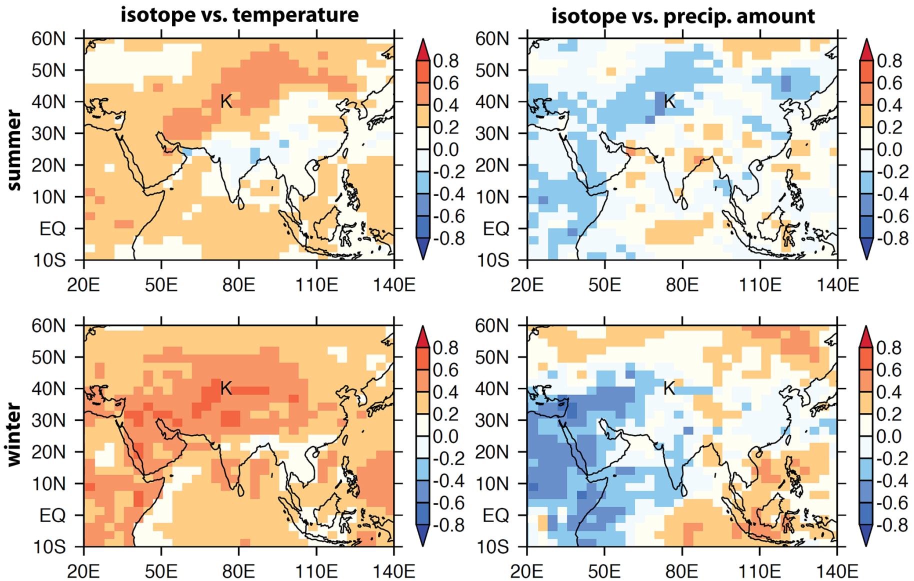

Figure 6. Spatial correlation coefficient (r) summer (April–September) and winter (October–March) $\delta^{18}O$ of precipitation at the Karakuli site (marked as K in the plots) with temperatures and precipitation amounts at each grid point from 1958 to 2009 using LMDZ4 simulations (Lee et al., 2012).

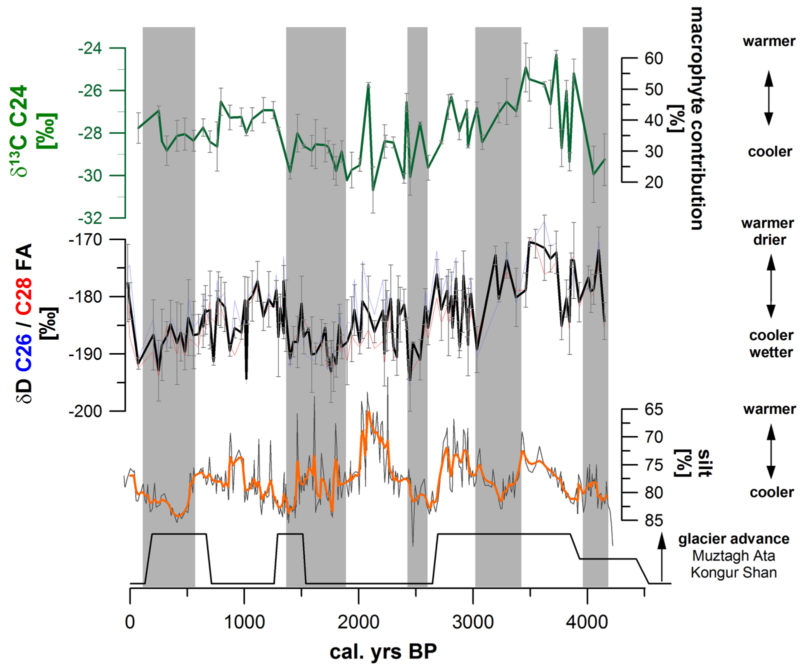

Figure 7. Summary of organic geochemical results from this study in context with silt contents of the same sediment core (Liu et al., 2014; orange line: 5-point weighted average) and data of local glacier advances on basis of ^{10}Be-dating (Seong et al., 2009a; centers and widths of boxes mark the mean age and the error ranges of the events). Biomarker hydrogen isotopic data are presented as mean of triplicate measurements for the C_{26} (blue line) and C_{28} *n*-alkanoic acids (red line) as well as unweighted average of the two (thick black line, with 1σ error bars). Shaded areas are relatively cool and wet episodes, based on leaf wax isotopic data.

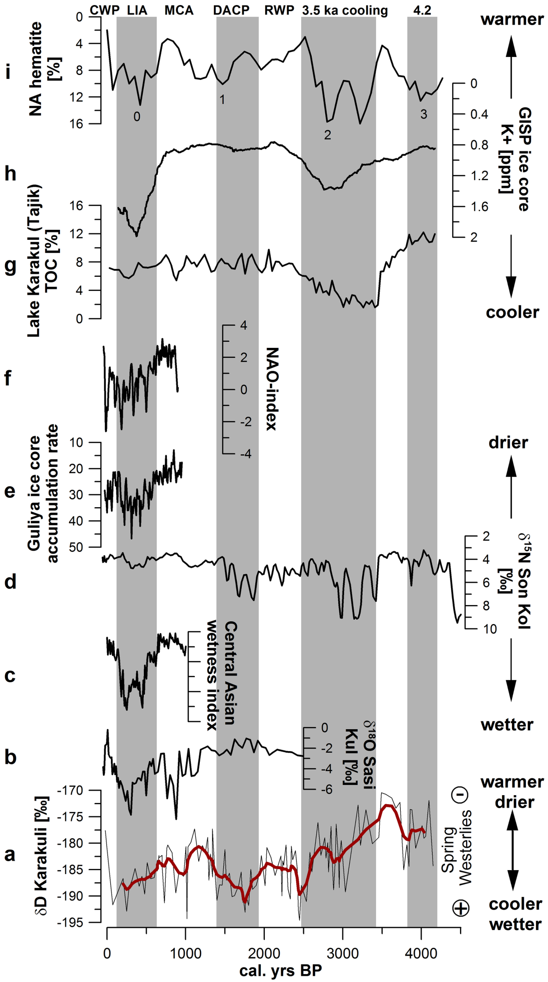

CPD
10, 4385–4424, 2014

Late Holocene paleoclimate in arid Central Asia

B. Aichner et al.

Figure 8. Comparison to local and Northern Hemispheric paleorecords. Shaded areas indicate relatively cool/wet episodes at Lake Karakuli; **(a)** δD of C_{26} and C_{28} *n*-alkanoic acids Lake Karakuli (this study); average values as in Fig. 8, red line: 5-point weighted average. **(b)** $\delta^{18}O$ Sasi Kul, Pamir, Tajikistan (Lei et al., 2014). **(c)** Central Asian wetness index (Chen et al., 2010). **(d)** $\delta^{15}N$ TN, Son Kol, Central Tien Shan, Kyrgyzstan (Lauterbach et al., 2014). **(e)** Guliya ice core accumulation rate (Thompson et al., 1997). **(f)** North Atlantic Oscillation index (Trouet et al., 2009). **(g)** TOC-contents large Lake Karakul, Pamir, Tajikistan (Mischke et al., 2010). **(h)** K^{+}GISP2 ice core (Mayewski et al., 1997). **(i)** Northern Atlantic Hematite grains indicate Northern Hemispheric cooling events "Bond-events" (Bond et al., 2001).

CPD
10, 4385–4424, 2014